

Chemical Biology

A Nitroxide-Tagged Platinum(II) Complex Enables the Identification of a DNA G-Quadruplex Binding Mode

Cui-Xia Xu^{+, [a]}, Xiaojun Zhang^{+, [b]}, Yi-Wei Zhou,^[a] Hanqiang Wang,^[a, c] Qian Cao,^[a] Yong Shen,^[a] Liang-Nian Ji,^[a] Zong-Wan Mao,^{*, [a]} and Peter Z. Qin^{*, [b]}

Abstract: We reported a novel strategy for investigating small molecule binding to G-quadruplexes (GQs). A newly synthesized dinuclear platinum(II) complex (Pt₂L) containing a nitroxide radical was shown to selectively bind a GQ-forming sequence derived from human telomere (hTel). Using the nitroxide moiety as a spin label, electron paramagnetic resonance (EPR) spectroscopy was carried out to investigate binding between Pt₂L and hTel GQ. Measurements indicated that two molecules of Pt₂L bind with one molecule of hTel

GQ. The inter-spin distance measured between the two bound Pt₂L, together with molecular docking analyses, revealed that Pt₂L predominately binds to the neighboring narrow and wide grooves of the G-tetrads as hTel adopts the antiparallel conformation. The design and synthesis of nitroxide tagged GQ binders, and the use of spin-labeling/EPR to investigate their interactions with GQs, will aid the development of small molecules for manipulating GQs involved in crucial biological processes.

Introduction

Guanine-rich oligonucleotides (either DNA or RNA) can form a unique stacked tetrad structure called G-quadruplex (GQ).^[1] In vitro biophysical studies have revealed that GQ-forming sequences can adopt a variety of topological conformations, classified as parallel, antiparallel or hybrid structures according to the strand orientations, which are distinct from duplexes or other nucleic acid conformations.^[2] GQs are known to exert important biological functions,^[3] and recent studies have revealed a significant presence of potential GQ-forming sites in genomes,^[4] as well as detected GQ conformations in vivo.^[5]

With their unique structure and biological function, GQs are recognized as potential drug targets,^[6] and various classes of small molecules targeting GQs are being investigated.^[7] In designing and developing compounds targeting GQs, detailed information on the mode of interaction between GQs and small

molecules is highly valuable. These interactions have been investigated by a variety of experimental (e.g., X-ray crystallography,^[8] NMR spectroscopy,^[9] optical spectroscopy,^[10] atomic force microscopy^[11] and optical tweezers^[12]) and computational (e.g., molecular dynamics simulations^[13]) approaches. However, our understanding on how small molecules interact with GQs remains far from complete.

In this study, we demonstrate a new strategy for investigating interactions between small molecules and GQs. Previously, the Mao group has synthesized and characterized series of mononuclear,^[14] dinuclear,^[15] trinuclear,^[16] and tetranuclear^[17] platinum(II) complexes that specifically bind to GQ forming sequences, stabilize GQ conformations, and inhibit telomerase activities. Especially, a dinuclear platinum(II) complex with quaternized trigeminal ligand, {[Pt(dien)]₂(dptmp)}(PF₆)₅ (dien: diethylenetriamine; dptmp: 4-[4,6-di(4-pyridyl)-1,3,5-(2-triazinyl)]-1-methylpyridine) has been reported, which acts as a selective GQ binder and telomerase inhibitor.^[15] In parallel, the Qin group has demonstrated that the technique of site-directed spin labeling, which utilizes electron paramagnetic resonance (EPR) spectroscopy to monitor behaviors of spin labels (e.g., stable nitroxide radicals) covalently attached to specific sites of biomolecules, can provide unique structural and dynamic information on nucleic acids and protein–nucleic acid complexes.^[18] Leveraging on these prior studies, we synthesized the first nitroxide tagged dinuclear platinum(II) complex (designated as Pt₂L, L: 4-([4,2':6',4''-terpyridin]-4'-yl)-N-(1-hydroxy-2,2,6,6-tetramethyl piperidin-4-oxyl)benzamide; Scheme 1). Using a combination of biochemical analyses, EPR, and molecular docking, we demonstrate that Pt₂L binds specifically to GQ-forming DNA sequence derived from the human telomere (hTel), and revealed details of its GQ binding mode.

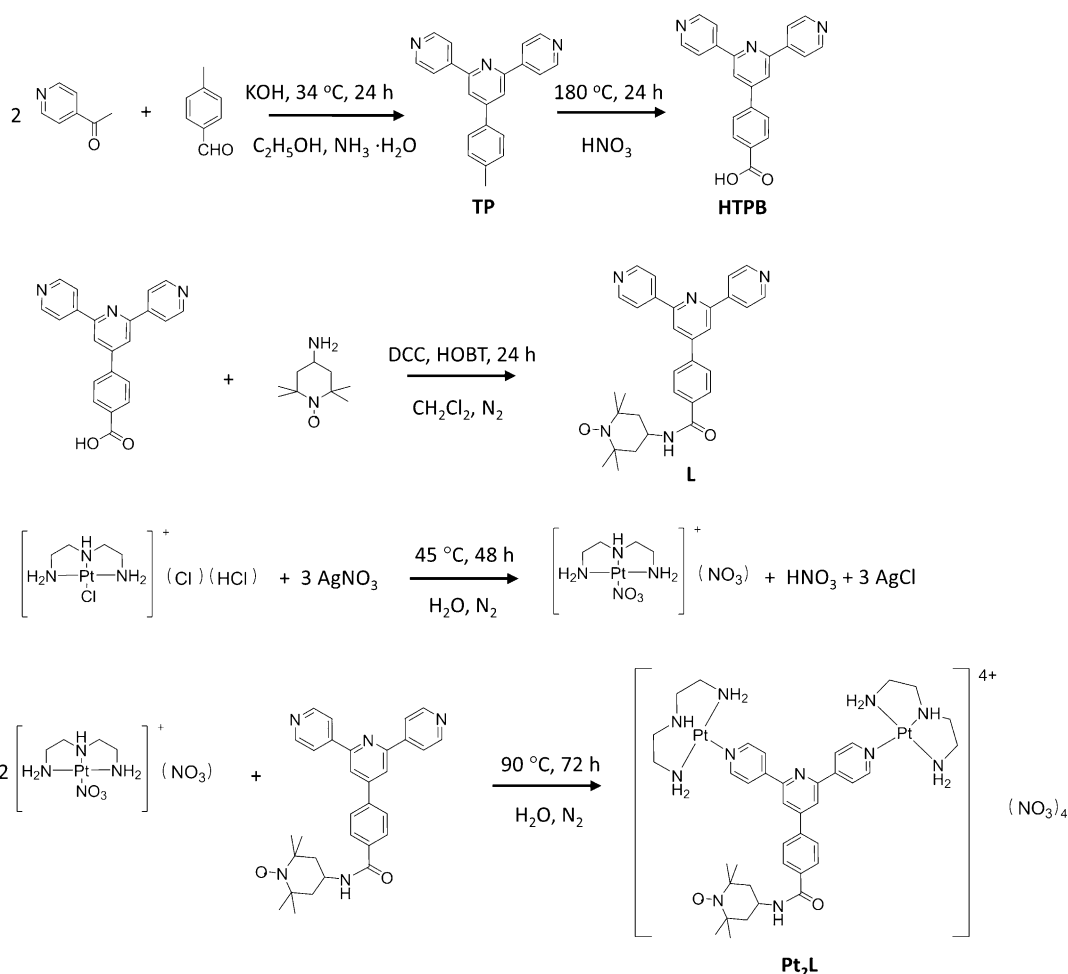
[a] Dr. C.-X. Xu,⁺ Y.-W. Zhou, H. Wang, Dr. Q. Cao, Dr. Y. Shen, Prof. Dr. L.-N. Ji, Prof. Dr. Z.-W. Mao
MOE Key Laboratory of Bioinorganic and Synthetic Chemistry
School of Chemistry and Chemical Engineering, Sun Yat-Sen University
Guangzhou, Guangdong, 510275 (P.R. China)
E-mail: cesmzw@mail.sysu.edu.cn

[b] Dr. X. Zhang,⁺ Prof. Dr. P. Z. Qin
Department of Chemistry, University of Southern California
Los Angeles, California, 90089 (USA)
E-mail: pzzq@usc.edu

[c] H. Wang
Current address: Department of Chemistry
The Chinese University of Hong Kong, Shatin
New Territories, Hong Kong (P.R. China)

[†] These authors contributed equally to this work.

Supporting information for this article is available on the WWW under <http://dx.doi.org/10.1002/chem.201504960>.



Scheme 1. The overall synthesis route of Pt₂L.

Results and Discussion

Synthesis, characterization and EPR spectroscopy of Pt₂L

To generate Pt₂L, we first synthesized L in three steps (Scheme 1). Starting with 1-(pyridin-4-yl)ethanone and 4-methylbenzaldehyde, 4'-(*p*-tolyl)-4,2':6',4''-terpyridine (TP) was synthesized as previously reported,^[19] which was then converted to 4-([4,2':6',4''-terpyridin-4'-yl])benzoic acid (HTPB).^[20] HTPB was coupled with a nitroxide radical (2,2,6,6-tetramethylpiperidine-1-oxyl)^[21] to form compound L (see the Experimental Section). The overall yield of L was 45% after HPLC purification. Pt₂L was then synthesized by incubating dechlorinated [Pt(dien)Cl]Cl·HCl and L in dark at 90 °C under constant stirring for 72 h. The overall yield of Pt₂L was approximately 71%. Successful syntheses of TP, HTPB and L were confirmed by mass spectrometry (Supporting Information, Section S1).

Continuous-wave EPR (cw-EPR) spectroscopy was then used to characterize the radical presented in Pt₂L. The measured cw-EPR spectrum showed the expected three-line pattern consistent with a ¹⁴N nitroxide (Figure 1A). Using a reported spin counting procedure,^[22] the ratio of electron spin to Pt₂L was determined to be 0.90 ± 0.18 from multiple measurements

(Figure 1B). Overall, the cw-EPR measurements confirmed that the nitroxide radical is preserved during synthesis of Pt₂L.

Pt₂L selectively binds to GQ and inhibit telomerase activity

We then examined the interactions between Pt₂L and various DNA sequences by measuring Pt₂L-dependent changes of melting temperature (ΔT_m) using a fluorescence resonance energy transfer (FRET) assay (Figure 2, Table 1). For the known GQ forming DNA sequence found in human telomere (hTel-21), a ΔT_m value of 29.6 °C was obtained, while L itself displayed little effect ($\Delta T_m < 1.0$ °C; Table 1, Figure S5 in the Supporting Information). This is comparable with previously characterized platinum(II) complexes that specifically bind and stabilize GQ (e.g., {Pt(dien)₂(dptmp)}(PF₆)₅, $\Delta T_m = 35.4$ °C^[15]). In contrast, with a duplex DNA, Pt₂L only induced a ΔT_m value of 1.5 °C, indicating little interaction between Pt₂L and duplex DNA. Furthermore, Pt₂L induced little changes in melting temperature for two other well-known GQ-forming sequences at promoter regions (*c-myc* and *bcl2*, Figure 2, Table 1). Overall, the data suggest that Pt₂L binds specifically to the hTel GQ, and can distinguish different GQ sequences.

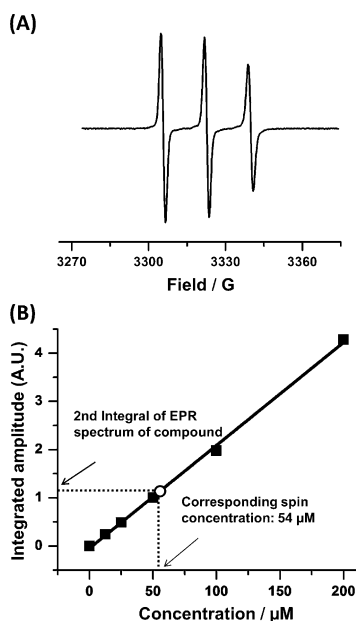


Figure 1. A) X-band cw-EPR spectrum of Pt₂L obtained in aqueous buffer. B) Spin counting. As shown, a set of TEMPO samples with known concentrations were measured (■), and linear fitting yielded a calibration curve [black line: integrated amplitude = 0.02135 × concentration (μM) − 0.04721]. Measurement was then carried out on a solution of 50 μM Pt₂L using the same experimental setting, and from the resulting integrated amplitude (○), the spin concentration was determined to be 54 μM, resulting in a ratio of electron spin-to-Pt₂L of 1.08.

We then evaluated the effect of Pt₂L towards human telomerase using a telomere repeat amplification protocol experiment (TRAP-LIG).^[16,23] The data show Pt₂L inhibited DNA elongation by telomerase in a concentration-dependent manner

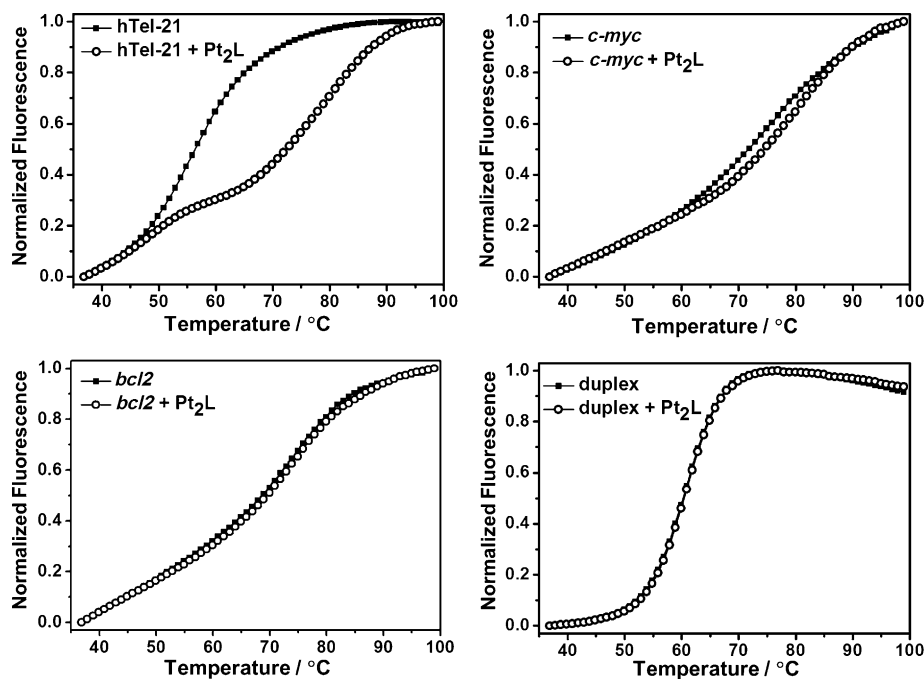


Figure 2. FRET-melting curves of DNA sequences (hTel-21, *c-myc*, *bcl2* and duplex) obtained in the absence and presence of Pt₂L. Data were obtained in 60 mM potassium cacodylate buffer (pH 7.4) with 400 nM DNA and 1.0 μM of Pt₂L.

Compound	ΔT_m [°C]			
	hTel-21	<i>c-myc</i>	<i>bcl2</i>	duplex
Pt ₂ L	29.6 ± 1.3	1.7 ± 0.3	0.8 ± 0.5	1.5 ± 0.2
L	0.5 ± 0.1	0	0	0

[a] Measured using a FRET assay. See the Experimental Section for details.

(Figure 3), with the IC₅₀ value determined to be 2.18 ± 0.024 μM. As such, Pt₂L can inhibit telomerase activities to a comparable degree as previously reported platinum(II) complexes.^[16]

EPR investigation of binding between Pt₂L and hTel GQ

Upon demonstrating that Pt₂L specifically interacts with hTel, we then investigated the binding stoichiometry between Pt₂L and hTel GQ using cw-EPR (Figure 4). The spectrum of the unbound Pt₂L showed three sharp lines, consistent with a small molecule undergoing rapid rotations (Figure 4A). Upon addition of hTel DNA, line-broadening was observed in the spectra (Figure 4A and Figure S6 in the Supporting Information), consistent with reduction of Pt₂L rotations upon formation of the Pt₂L-bound hTel complex that has a higher molecular weight. Using the ratio of the peak-to-peak amplitudes between the high-field line (H_{pp}) and the center line (C_{pp}) as a semi-quantitative parameter,^[24] spectral line-broadening upon increasing amount of hTel was found to saturate as the ratio of hTel to Pt₂L became ≥ 0.5 (Figure 4B, indicated by the arrow). This indicated a stoichiometry ratio of 2 in the complex, meaning

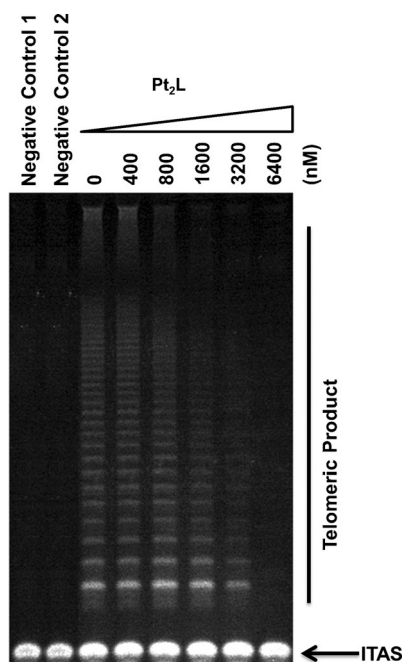


Figure 3. Pt₂L inhibited DNA elongation by human telomerase. As the concentration of Pt₂L increased, telomerase elongation products detected by PCR amplification clearly decreased, while PCR products from an internal control primer (ITAS, lowest band) remained constant. The negative controls showed that the elongation products required an active telomerase. See the Experimental Section for details.

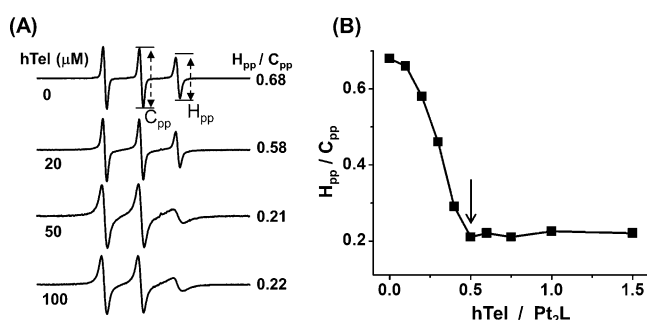


Figure 4. Stoichiometry of Pt₂L binding to hTel. A) Representative cw-EPR spectra measured upon titrating various amounts of hTel DNA with 100 μM of Pt₂L. Measurements were carried out in 100 mM NaCl and 10 mM Tris-HCl buffer (pH 7.4). B) Quantitation of hTel-dependent Pt₂L mobility changes.

two molecules of Pt₂L bind with one molecule of hTel GQ. The same conclusion was obtained from a Job-plot analysis of data measured using UV/Vis spectroscopy (Figure S7 in the Supporting Information).

Following characterization of binding stoichiometry, the inter-spin distance between the nitroxides of two Pt₂L within a Pt₂L-bound hTel complex was measured using double electron resonance (DEER) spectroscopy. In the presence of Na⁺, the measured DEER trace shows a clear decay (Figure 5A), reflecting dipolar interaction between two bound Pt₂L. The distance distribution profile obtained from analyzing the DEER trace shows a major population centered at 23 Å (Figure 5B). A minor population can also be observed at ap-

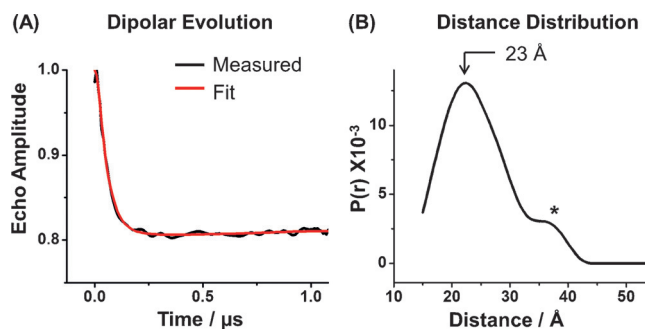


Figure 5. DEER measurement of two Pt₂L molecules bound to one hTel GQ. Measurements were carried out with 100 μM Pt₂L and 50 μM hTel in 100 mM NaCl, 10 mM Tris-HCl buffer (pH 7.4).

proximately 36 Å (Figure 5B, indicated by “*”), which may arise from experimental artifacts or alternative binding modes (see later).

Elucidating the mode of Pt₂L binding to hTel GQ

In parallel to DEER measurements, CD spectroscopy was carried out to assess conformations of Pt₂L-bound hTel GQ. It has been reported that antiparallel GQs typically show a positive band at 295 nm and a negative band at 265 nm,^[25] parallel GQs show a positive band at 275 nm and a small negative band at 240 nm,^[17a] and hybrid GQs show a strong positive band at 295 nm, a positive shoulder peak at 268 nm, and a small negative band at 240 nm.^[10a,26] Figure 6 shows measured CD spectra of hTel. As the concentration of Pt₂L increases, CD spectra measured in solutions of 10 mM Tris-HCl buffer (pH 7.4) without extra added metal ions show clear increases at the positive 295 nm band (Figure 6A), indicating formation of the antiparallel conformation. In the Na⁺ containing buffer, the spectrum obtained in the absence of Pt₂L shows a strong positive band at 295 nm and a negative band at 265 nm (Figure 6B, black line), which are prototypical antiparallel features. Upon titration of Pt₂L, the negative band at 265 nm initially became smaller, but stabilized as Pt₂L/hTel ratio ≥ 0.6. We interpreted this to indicate that a majority of hTel retains the antiparallel conformation. We also note that due to the positive 295 nm band, the presence of hybrid conformations cannot be excluded. However, all these spectra lack positive 275 nm band and negative 240 nm band, indicating an absence of the parallel conformation. Furthermore, the measured CD spectra show that the addition of L did not induce significant observable spectral changes (Figure S8 in the Supporting Information).

As CD spectra indicated that in the presence of sodium ions a majority of Pt₂L-bound hTel adopts an antiparallel topology, we carried out molecular docking analyses using the antiparallel structure of the hTel sequence determined by NMR spectroscopy (PDB ID: 143D).^[25a] Following procedures reported previously, Pt₂L was parameterized using Gaussian 09, then docked onto the fixed DNA structure using the Surflex-Dock suite.^[27]

Systematic search of docking parameters produced 58 unique models maintaining the proper chemical configuration

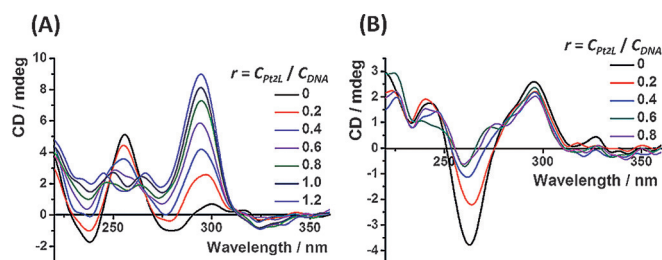


Figure 6. CD spectra of Pt₂L interacting with hTel. A) Spectra obtained in 10 mM Tris-HCl buffer (pH 7.4) without added metal salt. B) Spectra obtained in 100 mM NaCl and 10 mM Tris-HCl buffer (pH 7.4). All experiments were carried out with 3.0 μm hTel DNA, and the ratios (*r*) of Pt₂L to hTel are listed.

(Figure 7 and Section S5 in the Supporting Information). The first eight highest scored models dock nearly identically to the narrow groove formed by the G₃G₄G₅ and G₁₄G₁₅G₁₆ repeats (site I, Figure 7A; movie S1 in the Supporting Information). This favorable docking likely arises from a nice shape complementarity between the GQ groove and Pt₂L, together with electrostatic interaction between the platinum(II) arms and the phosphate groups of G₁₅, G₁₆, and T₁₇ (Figure 7A and C). In addition, 47 models dock at the wide groove formed by the G₃G₄G₅ and G₈G₉G₁₀ repeats (site II, Figure 7A; see also movie S1), and adopt variable conformations. The remaining three models docked in the groove formed by the G₈G₉G₁₀ and G₂₀G₂₁G₂₂ repeats, although further analyses and EPR experiments indicated that they do not represent a major conformation of Pt₂L bound at antiparallel GQ (see Section S5B in the Supporting Information). As such, molecular docking identified two Pt₂L binding sites in hTel GQ, which matches nicely with the stoichiometric ratio of 2 measured on the Pt₂L-bound hTel

complex (Figure 4 and Figure S7 in the Supporting Information).

Further analyses show that the inter-nitroxide distances between Pt₂L bound at sites I and II range between 7.8–33.4 Å (Figure 7B), and approximately 15% of them fall within 2.0 Å of the measured distance of 23 Å. Importantly, the average inter-nitroxide distances between models of the top two scored configurations is 22.8 Å (Figure 7C and movie S2 in the Supporting Information), matching nicely with the major population measured by DEER ($\langle r \rangle = 23$ Å, Figure 5). Furthermore, between the top 20 scored models found at site I and site II, the inter-nitroxide distance distribution falls nicely within the DEER measured profile (Figure 7D and Figure S9 in the Supporting Information). Together, we concluded that with the antiparallel GQ conformation, two Pt₂L molecules bind to the grooves of G-tetrads. One of them binds with high energy and well-defined configuration at the narrow groove formed by the G₃G₄G₅ and G₁₄G₁₅G₁₆ repeats (site I, Figure 7 and Figure S9A), while the other binds with relatively variable configurations to the wide groove formed by the G₃G₄G₅ and G₈G₉G₁₀ repeats (site II, Figure 7 and Figure S9B). The variable binding configurations at site II would present difficulty for other characterization techniques, such as X-ray crystallography or NMR spectroscopy. As such, the results exemplify the unique capability of combining spin-labeling/EPR and molecular modeling to investigate interactions between small molecules and GQs.

We note that the measured DEER distance profile shows a minor population at approximately 36 Å (indicated by "*" in Figure 5B), which is longer than all inter-nitroxide distances obtained from Pt₂L docked at the antiparallel GQ (Figure 7B). This minor population was found to vary in percentage in

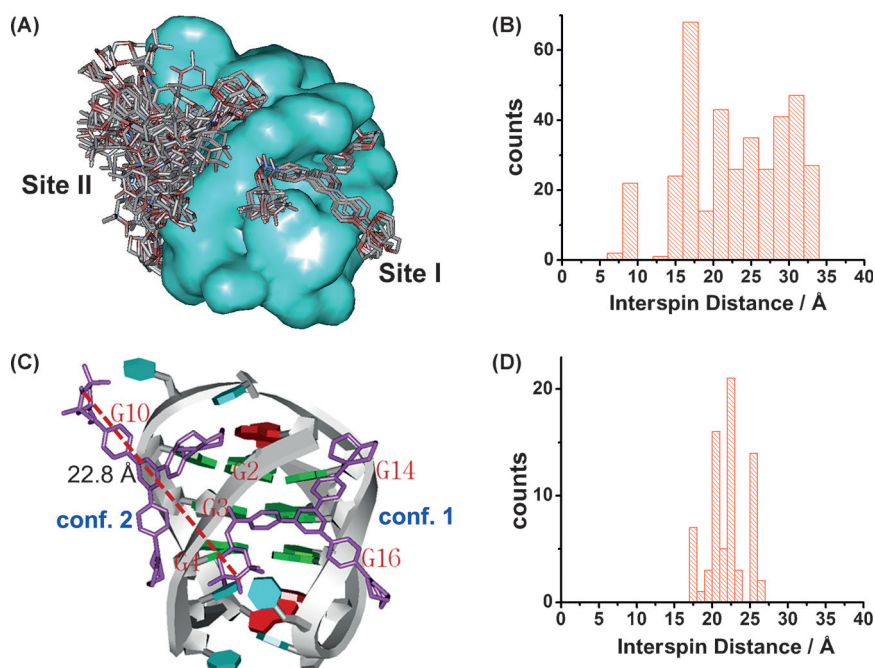


Figure 7. Pt₂L binding sites at antiparallel hTel GQ. A) Molecular docking revealed two major binding sites. B) Histogram of the inter-nitroxide distances between all Pt₂L docked at sites I and II. C) Representative views of the top two scored Pt₂L configurations. D) Histogram of the inter-nitroxide distances between the top 20 scored models residing at site I and site II. See the Supporting Information for additional details.

repeat measurements, and may be due partially to experimental artifacts. It may also arise from other GQ topologies. While CD measurements excluded the parallel topology in Pt₂L bound hTel (Figure 6), they did indicate the existence of other non-antiparallel topologies. However, docking using "3 + 1" hybrid GQ structures obtained for sequences similar but not identical to hTel failed to yield models consistent with all experimental EPR data (see Section S6 in the Supporting Information). Elucidating how Pt₂L binds to non-antiparallel GQ topologies will require further studies.

Conclusions

In summary, we successfully synthesized a nitroxide-tagged dinuclear platinum(II) complex Pt₂L, and demonstrate that it acts as a selective GQ stabilizer and telomerase inhibitor. EPR measurements, together with biochemical and computational analyses, revealed that Pt₂L binds to neighboring narrow and wide grooves of the G-tetrads in the antiparallel GQ. We also note that nitroxides afford a wide range of biological activities, including modulation of cellular redox processes. Nitroxides covalently linked to pharmacophores, including cisplatin, have been suggested to provide favorable pharmacology features.^[28] Taken together, work reported here on the GQ-specific platinum(II) complex establishes a new strategy to study interactions between small molecules and GQs, and may open up new opportunities for developing multifunctional platinum(II)-based complexes targeting GQs as well as other DNA structures.

Experimental Section

General

Dichloromethane (CH₂Cl₂, super dried with molecular sieves) and methyl alcohol (HPLC grade) were obtained from J&K Scientific Ltd. (Guangzhou, China). All the other reagents and solvents were chemical-pure grades, and were obtained commercially and used without further purification. All DNA oligonucleotides were produced by solid-phase chemical synthesis and obtained commercially.

Synthesis of Pt₂L ([Pt(dien)]₂L)(NO₃)₄, **L**: 4-([4,2':6',4''-terpyridin-4'-yl)-N-(1-hydroxy-2,2,6,6-tetramethylpiperidin-4-oxyl)-benzamide, **dien**: diethylenetriamine)

Synthesis of 4'-(p-tolyl)-4,2':6',4''-terpyridine (TP): TP was synthesized as previously reported.^[19] KOH·H₂O pellets (85% w/w, 1.32 g, 20 mmol) and NH₃·H₂O (35 mL, 25% v/v) were added to a solution that was under constant stirring and contained 1-(pyridin-4-yl)ethanone (2.42 g, 20 mmol) and 4-methylbenzaldehyde (1.20 g, 10 mmol) in EtOH (100 mL). After stirring at 34 °C for 24 h, the solution was incubated at 4 °C for 2 h. This process yielded pale yellow solids, which were collected by filtration and washed with cold EtOH (6 mL). The obtained raw product was recrystallized from EtOH to yield a white crystalline solid of TP (1.85 g, 57.2% yield). ESI-MS (CHCl₃) for C₂₂H₁₇N₃: *m/z* [TP + H⁺]⁺: anal. calcd 324.1, found 324.5; [2TP + H⁺]⁺: anal. calcd 647.2, found 647.3 (Figure S1 in the Supporting Information). Elemental analysis calcd (%) for C₂₂H₁₇N₃: C 81.71, H 5.30, N 12.99; found: C 81.62, H 5.36, N 12.93.

Synthesis of 4-([4,2':6',4''-terpyridin-4'-yl)benzoic acid (HTPB): HTPB was synthesized from TP using a previously reported method.^[20] TP in the solid form (6.46 g, 20 mmol) was added to concentrated HNO₃ (65%, v/v) in a Parr Teflon lined stainless steel vessel, and was heated at 180 °C for 24 h. The obtained mixture was cooled to room temperature, transferred to a big flask, stirred with 300 mL water, overnight, and then filtered and washed with water twice (2 × 10 mL). The final yellow product was dried under vacuum to give approximately 5.65 g of HTPB (80% yield). ESI-MS (DMF) for C₂₂H₁₅N₃O₂: *m/z* [HTPB + H⁺]⁺: anal. calcd 354.1, found 354.1; [HTPB + DMF + H⁺]⁺: anal. calcd 427.2, found 427.1 (Figure S2 in the Supporting Information). Elemental analysis calcd (%) for C₂₂H₁₅N₃O₂·3H₂O·HNO₃: C 56.17, H 4.71, N 11.91; found: C 56.43, H 4.59, N 12.31.

Synthesis of L (4-([4,2':6',4''-terpyridin-4'-yl)-N-(1-hydroxy-2,2,6,6-tetramethylpiperidin-4-oxyl)benzamide): L was synthesized using an amide condensation reaction,^[21] which coupled HTPB and a nitroxide radical (2,2,6,6-tetramethylpiperidine-1-oxyl). HTPB (0.20 g, 0.39 mmol), *N,N'*-dicyclohexylcarbodiimide (DCC, 0.09 g, 0.439 mmol), and 1-hydroxybenzotriazole (HOBT, 0.06 g, 0.44 mmol) were added into 10 mL of CH₂Cl₂, and stirred at room temperature for 1 h. Then 4-amino-2,2,6,6-tetramethylpiperidine-1-oxyl (4-amino-TEMPO, 0.062 g, 0.36 mmol) was added, and the mixture was stirred for approximately 16 h in dark under N₂. During this process, TLC was used to monitor reaction progress, and several aliquots of CH₂Cl₂ were added. The final product was purified using reverse-phase HPLC (0.89 g, 45% yield). ESI-MS (H₂O; positive mode) for C₃₁H₃₂N₅O₂: *m/z* [L + H⁺]⁺: anal. calcd 507.3, found 507.1 (Figure S3 in the Supporting Information); (negative mode) for C₃₁H₃₂N₅O₂: *m/z* [L - H⁺]⁻: anal. calcd 505.3, found 505.3 (Figure S4 in the Supporting Information). Elemental analysis calcd (%) for C₃₁H₃₂N₅O₂·3H₂O·HNO₃: C 70.95, H 6.53, N 13.35; found C 71.25, H 6.75, N 13.75.

Synthesis of {[Pt(dien)]₂L}(NO₃)₄ (Pt₂L): [Pt(dien)Cl]Cl·HCl and Pt₂L were synthesized according to a previously reported method.^[15] [Pt(dien)Cl]Cl·HCl (37 mg, 0.10 mmol) and AgNO₃ (34 mg, 0.20 mmol) were mixed in water (5.0 mL) and stirred in a stoppered flask under N₂ for 48 h at 45 °C. The mixture was then filtered to remove AgCl. The obtained pale yellow solution was transferred to another flask, then L (25 mg, 0.05 mmol) was added to the solution, and the mixture was stirred in dark at 90 °C until L disappeared (usually in approximately 72 h). The reaction mixture was then filtered and concentrated to approximately 0.5 mL. Approximately 70 mL EtOH was added to this solution, yielding a large amount of pale solid precipitant, which was collected using filtration and dried under vacuum (52.4 mg, 71% yield). Elemental analysis calcd (%) for {[Pt(dien)]₂L}(NO₃)₄·7H₂O: C 32.50, H 4.76, N 14.58; found: C 32.48, H 4.71, N 14.11.

DNA melting measurements using a fluorescence resonance energy transfer assay

Fluorescently labeled DNA oligonucleotides employed in FRET assays were:

- hTel-21: 5'-FAM-[GGGTTAGGGTT AGGGTTAGGG]-TAMRA-3'
- *c-myc*: 5'-FAM-[TGGGGAGGGT GGGGAGGGTG GGGGAAGG]-TAMRA-3'
- *bcl2*: 5'-FAM-[AGGGGCGGGC GCGGGAGGAA GGGGCGGGGA GCGGGGCTG]-TAMRA-3'
- duplex: 5'-FAM-[TATAGCTATA-HEG-TATAGCTATA]-TAMRA-3'

FAM: 6-carboxyfluorescein; TAMRA: 6-carboxy-tetramethylrhodamine; HEG linker: $[-(CH_2-CH_2-O)_2]$. The oligonucleotides were synthesized and HPLC purified by Shanghai Sangon, China.

For each measurement, a 50 μM stock of fluorescently labeled DNA oligonucleotides in water was made, and then diluted to 0.8 μM in a buffer of 60 mM potassium cacodylate, 10 mM Tris-HCl (pH 7.4). The DNA was annealed by heating at 95 °C for 5 min, then slowly cooled to room temperature and incubated overnight. Each sample was measured in a total volume of 20 μL , with the final concentration of DNA being 0.5 μM and small molecules (L or Pt₂L) being 1.0 μM . Melting curves were obtained using a Roche Light-Cycler 2.0 real-time PCR machine. Fluorescence data were recorded with an excitation wavelength at 470 nm, detection wavelength at 530 nm, at intervals of 1 °C during a temperature range of 37–99 °C, with each temperature being maintained for 30 s. Data analysis was carried out with Origin 8.0 (OriginLab Corp.).

Telomere-repeat amplification protocol assays

Materials (dNTP mix, RNase inhibitor, and Taq polymerase) were obtained from TaKaRa Biotechnology. DNA oligonucleotide primers were synthesized and PAGE purified by Invitrogen Technology, Shanghai, China. The primer sequences are: TS, 5'-AATCCGTCGA GCAGATT-3'; ACX, 5'-GCGCGCTTA CCCTACCC TTACCCTAAC-3'; NT, 5'-ATCGCTTCTC GGCCTTT-3'; and TSNT, 5'-AATCCGTCGA GCA-GAGTTAA AAGGCCGAGA AGCGAT-3'. The experiments included three steps.

Step 1: primer elongation by telomerase in the presence of Pt₂L: Telomerase extract was prepared from HeLa cells using the NP-40 lysis buffer, which contained 10 mM Tris-HCl, pH 8.0, 1.0 mM MgCl₂, 1.0 mM ethylene glycol tetraacetic acid (EGTA), 1.0% NP-40, 0.25 mM sodium deoxycholate, 10% glycerol, 150 mM NaCl, 0.1 mM phenylmethanesulfonylfluoride (PMSF) and 5.0 mM β -mercaptoethanol (β -ME). Each reaction was carried out in a volume of 50 μL . The reaction mixture included 5.0 μL of 10 \times TRAP buffer, 1.0 μL of 0.05 $\mu\text{g}\mu\text{L}^{-1}$ BSA, 4.0 μL of 2.5 mM dNTP mix, 1.0 μL of 100 $\text{ng}\mu\text{L}^{-1}$ TS primer, 0.5 μL of 2 $\text{U}\mu\text{L}^{-1}$ RNase inhibitor, 1.0 μL telomerase extract (obtained from ~500 cells), 32.5 μL diethyl pyrocarbonate-treated (DEPC) water, and 5.0 μL of Pt₂L at the desired concentration. The reaction mixture was transferred to a thermal cycler (Bio-Rad S1000, USA), then incubated at 30 °C for 30 min, 94 °C for 10 min, and a final maintenance temperature of 20 °C. A number of negative controls were included. Negative control 1: telomerase was heated inactivated by incubation at 85 °C for 10 min prior to primer elongation; negative control 2: telomerase was omitted, and the reactions were carried out using 1.0 μL lysis buffer instead of 1.0 μL telomerase extract; negative control 3: Pt₂L was omitted, and the reactions were carried out using 5.0 μL of DEPC-treated water instead of the Pt₂L complex.

Step 2: removal of Pt₂L: The QIA quick nucleotide purification kit (Qiagen, 28304) was used to purify the elongated products and to remove Pt₂L according to the manufacturer's instructions. As reported, ethanol was found to inhibit the PCR amplification. To avoid the inhibition effect of residual ethanol in the kit, the final samples eluted in water were freeze-dried.

Step 3: PCR amplification: PCR was carried out to amplify the telomerase elongation products. For each reaction the purified elongation products were dissolved in 37.6 μL water, then mixed with 5.0 μL 10 \times TRAP buffer (200 mM Tris-HCl, pH 8.3, 15 mM MgCl₂, 630 mM KCl, 0.5% Tween-20 and 10 mM EGTA in DEPC-treated water), 1.0 μL of 5.0 $\mu\text{g}\mu\text{L}^{-1}$ BSA, 4.0 μL of 2.5 mM dNTP mix, 1.0 μL of 100 $\text{ng}\mu\text{L}^{-1}$ TS primer, 1.0 μL of primer mix (100 $\text{ng}\mu\text{L}^{-1}$ ACX reverse primer, 100 $\text{ng}\mu\text{L}^{-1}$ NT primer, and 4.0 \times 10⁻¹⁴ M TSNT internal

control primer), and 0.4 μL of 5 $\text{U}\mu\text{L}^{-1}$ Taq polymerase. The mixtures were incubated at 94 °C for 90 s, then subjected to 30 cycles of PCR (94 °C for 30 s, 52 °C for 30 s and 72 °C for 45 s). The PCR products were separated on 8.0% polyacrylamide gels, run at approximately 250 V for 100 min. The final gels were stained with 10000 \times gel red (Biotium, USA) for approximately 15 min, then visualized under UV illumination (Gel image system, Tanon 1600, China).

Continuous-wave EPR spectroscopy

The hTel DNA (5'-AGGGTTAGGGT TAGGGTTAGGG-3') was obtained commercially (Integrated DNA Technology, Coralville) and purified by HPLC.^[18c] To anneal the DNA, hTel DNA was first heated at 95 °C for 5 min, then appropriate buffer was added to a final concentration of 100 mM NaCl, 10 mM Tris-HCl (pH 7.4). The mixture was cooled to room temperature and then incubated at 4 °C overnight. To analyze the binding of Pt₂L to hTel, the desired amount of annealed hTel was incubated with 100 μM of Pt₂L in a solution of 100 mM NaCl, 10 mM Tris-HCl at pH 7.4. Incubations were carried out for 30 min at room temperature, following which cw-EPR spectra were acquired.

Each cw-EPR spectrum was obtained using a 5 μL sample loaded in a round glass capillary (0.6 mm i.d. \times 0.8 mm o.d., Vitrocom, Inc., Mountain Lakes) sealed at one end. Measurements were carried out at room temperature on an X-band Bruker EMX spectrometer using an ER4119HS resonator. The incident microwave power was 2 mW, and the field modulation was 1 G at a frequency of 100 kHz. Each spectrum was acquired with 512 points, corresponding to a spectral range of 100 G. All spectra were corrected for background and baseline, and if needed, normalized following reported procedures.^[22]

Double electron electron resonance spectroscopy

Measurements were carried out on samples of Pt₂L-bound hTel. To prepare a sample, appropriate amount of Pt₂L and annealed hTel DNA (see above) were mixed in a solution containing 100 mM NaCl and 10 mM Tris-HCl (pH 7.4). The mixture was incubated at room temperature for 30 min, and then glycerol solution with the proper amount of salt was added to obtain a sample with a final concentration of 100 mM NaCl, 10 mM Tris-HCl (pH 7.4) and 50% glycerol (v/v). The sample was immediately loaded into a quartz capillary and flash frozen by submerging in liquid nitrogen, and then used immediately for measurement.

DEER measurements were carried out at 78 K on a Bruker ELEXSYS E580 X-band spectrometer equipped with a MD4 resonator. Previously reported acquisition parameters and procedures^[29] were used with slight modifications ($d_1 = 200$ ns instead of 128 ns). Specifically, a dead-time-free four-pulse scheme was used,^[30] with the pump pulse frequency set at the center of the nitroxide spectrum and the observer frequency at approximately 70 MHz higher. The observer π pulse was 32 ns, and the pump π pulse was optimized using a nutation experiment, usually set at 16 ns. The video bandwidth was fixed at 20 MHz. The shot repetition time was set at 1000 μs . Accumulation time in each measurement was approximately 24 h with 100 shots per point. Inter-spin distance distributions were computed from the resulting dipolar evolution data using DEER analysis 2013.^[31]

Circular dichroism spectroscopy

Circular dichroism measurements were carried out using the hTel DNA (5'-AGGGTTAGGGT TAGGGTTAGGG-3'). The DNA was synthe-

sized and purified by denaturing gel by the vendor (Shanghai Sangon, Inc., China). CD spectra were measured over a wavelength range of 220–360 nm at room temperature using a J-810 spectropolarimeter (JASCO, Japan), with 1 cm optical path-length, and 200 nm min⁻¹ scan speed. The DNA sample was dissolved in 10 mM Tris-HCl (pH 7.4) containing either no extra added metal ion or 100 mM NaCl. Previously reported experimental procedures were used,^[16] and data analysis was performed using Origin 8.0 (OriginLab Corp.).

Molecular docking

Pt₂L was optimized in geometry at the B3LYP/6–31G* level (B3LYP/LanL2DZ for Platinum)^[27a] using the Gaussian 09 program.^[27b] ESP charges were calculated at the same level.

Molecular docking was carried out using the Surflex Dock program in Sybyl-X 2.0 package. NMR-determined structures of antiparallel (PDB ID: 143D^[25a]) and 3 + 1 hybrid (PDB ID: 2JPZ^[32] and 2HY9^[33]) GQs were obtained from the protein data bank (PDB). Each round of docking examined binding of Pt₂L (parameter optimized as described above) to a fixed target DNA represented by model 1 of a particular GQ topology, following procedures similar to those reported previously.^[34] Briefly, the protocol was first generated by the automatic mode, then the threshold and bloat parameters were varied according to an orthogonal experimental design (threshold: 0.1–0.7, increment 0.2; bloat: 0–10, increment 2). The additional starting conformation was set to 20 and other parameters were set as default.

For each GQ topology, a total of 480 docked Pt₂L models were scored and retrieved. Two additional processing steps were carried out to produce the ensemble of unique docked models maintaining the proper chemical configuration. First, a requirement that the length of each of the eight Pt–N bonds must fall between 1.9 and 2.3 Å was imposed. This removed many of the models in which one or both of the Pt arms were distorted as the program attempted to achieve a better docking score. In addition, redundant models, defined as those have identical coordinates but were obtained from different search parameters, were eliminated.

Acknowledgements

This work is supported in part by the National Science Foundation (CHE-1213673, CHE-1156836), the National Institute of Health (RR028992), National Natural Science Foundation of China (Nos. 21172274, 21328101 and 21231007), the Ministry of Education of China (Nos. IRT1298 and 313058), the National Basic Research Program of China (973 Program Nos. 2014CB845604 and 2015CB856301), and the Fundamental Research Funds for the Central Universities.

Keywords: EPR spectroscopy • G-quadruplexes • molecular docking • nitroxide • platinum(II) complexes

- [1] J. B. Chaires, D. Graves, *Quadruplex Nucleic Acids* **2013**, 330.
- [2] a) J. Dai, M. Carver, D. Yang, *Biochimie* **2008**, 90, 1172–1183; b) A. T. Phan, *FEBS J.* **2010**, 277, 1107–1117.
- [3] H. J. Lipps, D. Rhodes, *Trends Cell Biol.* **2009**, 19, 414–422.
- [4] J. L. Huppert, S. Balasubramanian, *Nucleic Acids Res.* **2005**, 33, 2908–2916.
- [5] a) G. Biffi, D. Tannahill, J. McCafferty, S. Balasubramanian, *Nat. Chem.* **2013**, 5, 182–186; b) G. Biffi, M. Di Antonio, D. Tannahill, S. Balasubramanian, *Nat. Chem.* **2013**, 6, 75–80.

- [6] S. Balasubramanian, L. H. Hurley, S. Neidle, *Nat. Rev. Drug. Discov.* **2011**, 10, 261–275.
- [7] a) A. Arola, R. Vilar, *Curr. Top. Med. Chem.* **2008**, 8, 1405–1415; b) S. N. Georgiades, N. H. Abd Karim, K. Suntharalingam, R. Vilar, *Angew. Chem. Int. Ed.* **2010**, 49, 4020–4034; *Angew. Chem.* **2010**, 122, 4114–4128; c) S. Müller, R. Rodriguez, *Expert Rev. Clin. Phar.* **2014**, 7, 663–679; d) C. Zhao, L. Wu, J. Ren, Y. Xu, X. Qu, *J. Am. Chem. Soc.* **2013**, 135, 18786–18789.
- [8] G. W. Collie, R. Promontorio, S. M. Hampel, M. Micco, S. Neidle, G. N. Parkinson, *J. Am. Chem. Soc.* **2012**, 134, 2723–2731.
- [9] a) C. E. Kaiser, V. Gokhale, D. Yang, L. H. Hurley, *Top. Curr. Chem.* **2012**, 330, 1–21; b) W. J. Chung, B. Heddi, F. Hamon, M. P. Teulade-Fichou, A. T. Phan, *Angew. Chem. Int. Ed.* **2014**, 53, 999–1002; *Angew. Chem.* **2014**, 126, 1017–1020.
- [10] a) A. I. Karsiotis, N. M. a. Hessari, E. Novellino, G. P. Spada, A. Randazzo, M. Webba da Silva, *Angew. Chem. Int. Ed.* **2011**, 50, 10645–10648; *Angew. Chem.* **2011**, 123, 10833–10836; b) A. Shivalingam, M. A. Izquierdo, A. L. Marois, A. Vysniauskas, K. Suhling, M. K. Kuimova, R. Vilar, *Nat. Commun.* **2015**, 6, 8178; c) R. Tippana, W. Xiao, S. Myong, *Nucleic Acids Res.* **2014**, 42, 8106–8114; d) L. N. Zhu, B. Wu, D. M. Kong, *Nucleic Acids Res.* **2013**, 41, 4324–4335; e) K.-W. Zheng, D. Zhang, L. X. Zhang, Y. H. Hao, X. Zhou, Z. Tan, *J. Am. Chem. Soc.* **2011**, 133, 1475–1483.
- [11] A.-M. Chiorcea-Paquim, P. V. Santos, R. Eritja, A. M. Oliveira-Brett, *Phys. Chem. Chem. Phys.* **2013**, 15, 9117–9124.
- [12] a) D. Koirala, S. Dhakal, B. Ashbridge, Y. Sannohe, R. Rodriguez, H. Sugiyama, S. Balasubramanian, H. Mao, *Nat. Chem.* **2011**, 3, 782–787; b) P. M. Yangyuru, M. Di Antonio, C. Ghimire, G. Biffi, S. Balasubramanian, H. Mao, *Angew. Chem. Int. Ed.* **2015**, 54, 910–913; *Angew. Chem.* **2015**, 127, 924–927.
- [13] S. M. Haider, S. Neidle, *Biochem. Soc. Trans.* **2009**, 37, 583–588.
- [14] a) J.-T. Wang, Y. Li, J.-H. Tan, L.-N. Ji, Z.-W. Mao, *Dalton Trans.* **2011**, 40, 564–566; b) J.-T. Wang, X.-H. Zheng, Q. Xia, Z.-W. Mao, L.-N. Ji, K. Wang, *Dalton Trans.* **2010**, 39, 7214–7216.
- [15] C.-X. Xu, Y.-X. Zheng, X.-H. Zheng, Q. Hu, Y. Zhao, L.-N. Ji, Z.-W. Mao, *Sci. Rep.* **2013**, 3.
- [16] C. X. Xu, Y. Shen, Q. Hu, Y. X. Zheng, Q. Cao, P. Z. Qin, Y. Zhao, L. N. Ji, Z. W. Mao, *Chem. Asian J.* **2014**, 9, 2519–2526.
- [17] a) X.-H. Zheng, H.-Y. Chen, M.-L. Tong, L.-N. Ji, Z.-W. Mao, *Chem. Commun.* **2012**, 48, 7607–7609; b) X.-H. Zheng, Y.-F. Zhong, C.-P. Tan, L.-N. Ji, Z.-W. Mao, *Dalton Trans.* **2012**, 41, 11807–11812; c) X.-H. Zheng, Q. Cao, Y.-L. Ding, Y.-F. Zhong, G. Mu, P. Z. Qin, L.-N. Ji, Z.-W. Mao, *Dalton Trans.* **2015**, 44, 50–53.
- [18] a) Y. Ding, P. Nguyen, N. S. Tangprasertchai, C. V. Reyes, X. Zhang, P. Z. Qin, in *Electron Paramagnetic Resonance*, RSC, **2015**, pp. 122–147; b) G. Z. Sowa, P. Z. Qin, in *Progress in Nucleic Acid Research and Molecular Biology* (Ed.: P. M. Conn), Academic Press, **2008**, pp. 147–197; c) P. Z. Qin, I. S. Haworth, Q. Cai, A. K. Kusnetzov, G. P. G. Grant, E. A. Price, G. Z. Sowa, A. Popova, B. Herreros, H. He, *Nat. Protoc.* **2007**, 2, 2354–2365.
- [19] B. Tang, F. Yu, P. Li, L. Tong, X. Duan, T. Xie, X. Wang, *J. Am. Chem. Soc.* **2009**, 131, 3016–3023.
- [20] a) J. Kim, B. Chen, T. M. Reineke, H. Li, M. Eddaoudi, D. B. Moler, M. O’Keeffe, O. M. Yaghi, *J. Am. Chem. Soc.* **2001**, 123, 8239–8247; b) Z. Lin, T. J. Emge, R. Warmuth, *Chem. Eur. J.* **2011**, 17, 9395–9405.
- [21] C. Su Lim, D. Won Kang, Y. Shun Tian, J. Hee Han, H. Lim Hwang, B. Rae Cho, *Chem. Commun.* **2010**, 46, 2388–2390.
- [22] X. Zhang, P. Cekan, S. T. Sigurdsson, P. Z. Qin, *Methods Enzymol.* **2009**, 469, 303–328.
- [23] a) J. Reed, M. Gunaratnam, M. Beltran, A. P. Reszka, R. Vilar, S. Neidle, *Anal. Biochem.* **2008**, 380, 99–105; b) A. De Cian, G. Cristofari, P. Reichenbach, E. De Lemos, D. Monchaud, M.-P. Teulade-Fichou, K. Shin-Ya, L. Lacroix, J. Lingner, J.-L. Mergny, *Proc. Natl. Acad. Sci. USA* **2007**, 104, 17347–17352.
- [24] P. Qin, S. Butcher, J. Feigon, W. Hubbell, *Biochemistry* **2001**, 40, 6929–6936.
- [25] a) Y. Wang, D. J. Patel, *Structure* **1993**, 1, 263–282; b) R. Giraldo, M. Suzuki, L. Chapman, D. Rhodes, *Proc. Natl. Acad. Sci. USA* **1994**, 91, 7658–7662.
- [26] a) B. Fu, J. Huang, L. Ren, X. Weng, Y. Zhou, Y. Du, X. Wu, X. Zhou, G. Yang, *Chem. Commun.* **2007**, 3264–3266; b) B. Fu, D. Zhang, X. Weng, M. Zhang, H. Ma, Y. Ma, X. Zhou, *Chem. Eur. J.* **2008**, 14, 9431–9441.

- [27] a) N. S. Venkataramanan, S. Ambigapathy, H. Mizuseki, Y. Kawazoe, *J. Phys. Chem. B* **2012**, *116*, 14029–14039; b) Gaussian 09, Revision A.02, M. J. Frisch, G. W. Trucks, H. B. Schlegel, G. E. Scuseria, M. A. Robb, J. R. Cheeseman, G. Scalmani, V. Barone, B. Mennucci, G. A. Petersson, H. Nakatsuji, M. Caricato, X. Li, H. P. Hratchian, A. F. Izmaylov, J. Bloino, G. Zheng, J. L. Sonnenberg, M. Hada, M. Ehara, K. Toyota, R. Fukuda, J. Hasegawa, M. Ishida, T. Nakajima, Y. Honda, O. Kitao, H. Nakai, T. Vreven, J. A. Montgomery, Jr., J. E. Peralta, F. Ogliaro, M. Bearpark, J. J. Heyd, E. Brothers, K. N. Kudin, V. N. Staroverov, R. Kobayashi, J. Normand, K. Raghavachari, A. Rendell, J. C. Burant, S. S. Iyengar, J. Tomasi, M. Cossi, N. Rega, J. M. Millam, M. Klene, J. E. Knox, J. B. Cross, V. Bakken, C. Adamo, J. Jaramillo, R. Gomperts, R. E. Stratmann, O. Yazyev, A. J. Austin, R. Cammi, C. Pomelli, J. W. Ochterski, R. L. Martin, K. Morokuma, V. G. Zakrzewski, G. A. Voth, P. Salvador, J. J. Dannenberg, S. Dapprich, A. D. Daniels, Ö. Farkas, J. B. Foresman, J. V. Ortiz, J. Cioslowski, D. J. Fox, Gaussian, Inc. Wallingford CT, **2009**.
- [28] V. D. Sen, A. A. Terentiev, N. P. Konovalova, in *Nitroxides: Theory, Experiment and Applications* (Ed.: A. I. Kokorin), InTech, **2012**, pp. 385–406.
- [29] a) X. Zhang, C.-S. Tung, G. Z. Sowa, M. m. M. Hatmal, I. S. Haworth, P. Z. Qin, *J. Am. Chem. Soc.* **2012**, *134*, 2644–2652; b) X. Zhang, A. C. Dantas Machado, Y. Ding, Y. Chen, Y. Lu, Y. Duan, K. W. Tham, L. Chen, R. Rohs, P. Z. Qin, *Nucleic Acids Res.* **2014**, *42*, 2789–2797.
- [30] M. Pannier, S. Veit, A. Godt, G. Jeschke, H. W. Spiess, *J. Magn. Reson.* **2000**, *142*, 331–340.
- [31] G. Jeschke, V. Chechik, P. Ionita, A. Godt, H. Zimmermann, J. Banham, C. Timmel, D. Hilger, H. Jung, *Appl. Magn. Reson.* **2006**, *30*, 473–498.
- [32] J. Dai, M. Carver, C. PUNCHIHewa, R. A. Jones, D. Yang, *Nucleic Acids Res.* **2007**, *35*, 4927–4940.
- [33] J. Dai, C. PUNCHIHewa, A. Ambrus, D. Chen, R. A. Jones, D. Yang, *Nucleic Acids Res.* **2007**, *35*, 2440–2450.
- [34] H. Lai, Y. Xiao, S. Yan, F. Tian, C. Zhong, Y. Liu, X. Weng, X. Zhou, *Analyst* **2014**, *139*, 1834–1838.

 Received: December 10, 2015

Published online on February 4, 2016